Available online at www.sciencedirect.com

ScienceDirect

journal homepage: http://www.elsevier.com/locate/euprot

Multidimensional LC–MS/MS analysis of liver proteins in rat, mouse and human microsomal and S9 fractions

*Makan Golizeh, Christina Schneider, Leanne B. Ohlund, Lekha Sleno**

Université du Québec à Montréal (UQÀM), Chemistry Department/Pharmaqam, Montréal, QC, Canada

ARTICLE INFO

Article history:
Received 2 December 2014
Received in revised form
20 January 2015
Accepted 27 January 2015
Available online 11 February 2015

Keywords:
Multidimensional liquid chromatography
High resolution tandem mass spectrometry
Liver proteins
Microsomal fractions
S9 fractions
Cross-species analysis

ABSTRACT

Liver plays a key role in metabolism and detoxification, therefore analysis of its proteome is relevant for toxicology and drug discovery studies. To optimize for high proteome coverage, protein and peptide-level ion exchange fractionation were assessed using rat liver microsomes and S9 fractions. 2D-(SCX-RP)-LC–MS/MS analysis with peptide fractionation was subsequently employed for rat, mouse and human samples, yielding between 1400 and 1939 identified proteins, 58% of which were shared between species, and with relatively high sequence coverage. This rich dataset is specifically interesting for the toxicology community, and could serve as an excellent source for targeted assay development.

1. Introduction

Multidimensional liquid chromatography (MDLC) improves the separation of highly complex mixtures, and has been applied to proteomics, lipidomics and the analysis of natural compounds [1]. In both qualitative and quantitative proteomics, MDLC has proven to be a powerful tool to increase the coverage and sensitivity of protein profiling, as well as improving the accuracy and reproducibility of quantitative analysis [2,3]. Generally, compared to a 1D-chromatography, combining multiple chromatographic separations will enhance resolving power, limit of detection and dynamic range by significantly increasing peak capacity

Abbreviations: CATWAX, mixed-bed weak cation/weak anion exchange; FDR, false discovery rate; GO, gene ontology; HILIC, hydrophilic interaction chromatography; HLM, human liver microsomes; HLS, human liver S9 fraction; HRMS, high-resolution mass spectrometry; IDA, information-dependent acquisition; IMP, integral membrane protein; MDLC, multidimensional liquid chromatography; MLM, mouse liver microsomes; MLS, mouse liver S9 fraction; MSA, multiple sequence alignment; RLM, rat liver microsomes; RLS, rat liver S9 fraction; UHPLC, ultra-high-performance liquid chromatography; WAX, weak anion exchange; WCX, weak cation exchange.

* *Corresponding author at*: Department of Chemistry/Pharmaqam, Université du Québec à Montréal (UQÀM), P.O. Box 8888, Downtown Station, Montréal, QC H3C3P8, Canada. Tel.: +1 514 987 3000x1599; fax: +1 514 987 4054.
E-mail address: sleno.lekha@uqam.ca (L. Sleno).

http://dx.doi.org/10.1016/j.euprot.2015.01.003

[4]. Common LC techniques used in MDLC include high-pH and low-pH RP, anion or cation exchange, size-exclusion chromatography as well as hydrophilic interaction chromatography (HILIC) and affinity chromatography [5]. Orthogonality of separation is an important parameter for achieving a high peak capacity, thus most common examples include high-low pH RP-RP, strong cation exchange (SCX)-RP and HILIC-RP for expanding proteome coverage [6].

Ion-exchange chromatography is often used as a first dimension of separation. In principle, there are two modes of ion exchange separation: cation and anion exchange. Combining SCX with RP chromatography offers high orthogonality, as SCX has a high loading capacity while RP can achieve high resolution separations amenable to LC–MS analysis and both involve different mechanisms [7]. It is also possible to combine two complementary ion (cation and anion) exchange columns either in tandem or as part of a mixed-bed column for increased separation efficiency. Havugimana et al. highlighted, in 2007, an improved number of identified proteins and higher quality of proteomics data using a "dual-column" approach with weak anion exchange (WAX) column coupled to a moderate cation exchange (MCX) column for the analysis of mouse heart cytosol [8]. Motoyama et al. published, in the same year, a study with increased number of identified proteins in yeast using a mixed-bed weak cation/weak anion exchange (CATWAX) column [9]. The use of a 3D-LC–MS approach incorporating CATWAX and SCX for protein and peptide fractionation was also reported by Zhang et al. to facilitate in-depth protein identification in mouse mammary tumor 4T1 cell lysate [10].

Liver plays a crucial role in the metabolism of xenobiotics through numerous enzymes involved in detoxification. A significant portion of these enzymes can be enriched in the microsomal fraction during subcellular fractionation [11] and therefore liver microsomes are often used in drug metabolism studies. Microsomes are rich sources of membrane proteins from endoplasmic reticulum, plasma membrane, mitochondria, and Golgi apparatus [12]. Integral membrane proteins (IMPs) represent the most pharmaceutically useful class of receptors [13], the targets of 70–80% of all known drugs [12], having strong implications in cell survival [14]. However, they are often tightly bound or physically integrated into the membrane and thus pose technical difficulties for proteomic analysis [15]. Liver S9 fraction, a mixture of microsomal and cytosolic fractions, is another important sample to study as it and is also often employed in toxicological and drug metabolism studies [16]. Since an important goal in proteomics research aims at determining post-translational modifications (including covalent binding from reactive endogenous/exogenous species) [17], an ideal method would achieve very high sequence coverage of all potentially targeted proteins.

We previously reported [18] an approach for the proteomic analysis of rat liver microsomes examining different combinations of proteases and solubilizing agents using single digestion, serial dual digestion and parallel dual digestion workflows. An SDS-assisted parallel tryptic–peptic dual digestion method exhibited the highest proteome coverage with 768 proteins identified at 1% global false discovery rate (25% average protein sequence coverage) with a high proportion (19.3%) of integral membrane proteins. To further enhance proteome coverage, the present study compares several MDLC-based separations of rat liver microsomal and S9 fractions incorporating both protein-level and peptide-level fractionation. Four strategies were devised to optimize the proteomic analysis of rat liver samples combining ion exchange with reverse-phase chromatography coupled to high-resolution quadrupole-time-of-flight (QqTOF) mass spectrometry. The approach with the best overall performance was then selected to carry out a cross-species proteomics comparison of rat, mouse and human liver fractions.

The main goal of this work was to improve the proteome coverage for samples of specific interest to drug metabolism and toxicology research, relatively rich in membrane proteins, where achieving high sequence coverage is particularly challenging. The increased coverage of individual proteins enhances the confidence of their detection with a higher number of peptides per protein, therefore yielding a better potential for accurate protein quantitation. For instance, this study is particularly useful for applications involving the absolute quantitation and expression profiling of cytochrome P450 and UDP-glucuronosyltransferase enzymes [19–21]. Moreover, when specific protein modifications are studied, higher protein coverage would increase the chances of seeing such modifications in complex samples.

2. Materials and methods

2.1. *Materials*

Male Sprague-Dawley rat, male ICR/CD-1 mouse, and human (M-50 donor) pooled liver microsomes (20 mg/ml protein) were purchased from Celsis In Vitro Technologies (Baltimore, MD). Rat liver S9 fractions (37.5 mg/ml protein) were from Moltox (Boone, NC), while male CD-1 mouse and human liver S9 fractions (20 mg/ml protein) were purchased from BD Biosciences (Franklin Lakes, NJ). Sequencing-grade modified trypsin was obtained from Promega (Madison, WI). Porcine gastric mucosa pepsin and all other chemical reagents were purchased from Sigma–Aldrich (St. Louis, MO). HPLC-grade ACN, methanol and isopropanol were from Caledon (Georgetown, ON), and ultrapure water was from a Millipore Synergy UV system (Billerica, MA).

2.2. *Sample digestion*

Liver microsomes or S9 fractions (0.5–0.6 mg protein) were solubilized with a 2% SDS solution (1:1, v/v), heated at 95 °C for 3 min, and diluted with 0.1 M ammonium bicarbonate (pH 8.5) to 200 μl. Reductive alkylation was performed using DTT (2.5 mM, 10 min, 25 °C) and iodoacetamide (5 mM, 30 min, 37 °C, dark). Samples were diluted with 150 μl of 0.1 M ammonium bicarbonate (pH 8.5) for trypsin digestions or 0.2% TFA in 20% methanol for pepsin digestions, and incubated at a 1:50 (w/w) enzyme:protein ratio for 18 h, at 37 °C for trypsin and 25 °C for pepsin with an additional 15 μl of 10% TFA prior to adding pepsin samples to maintain the required acidic digestion conditions (pH 1.5–2). CATWAX protein fractions were reconstituted in 150 μl of 0.1 M ammonium bicarbonate

(pH 8.5), denatured and digested using 5 μg of either enzyme. Digestion was quenched by adding 50 μl of 1% formic acid for trypsin or 1% ammonium hydroxide for pepsin. Samples were then diluted with 500 μl H_2O prior to solid-phase extraction (SPE) on a 1 cc (30 mg) OASIS HLB cartridge (Waters, Milford, MA), eluting with 100% methanol (1 ml). Resulting samples were evaporated to dryness under vacuum (Thermo Fisher Scientific Universal Vacuum System, Asheville, NC) and stored at −30 °C.

2.3. Protein fractionation

Solubilized protein samples (1.4 mg total) were diluted with buffer A (see below) to have a total volume of 280 μl (5 mg/ml), sonicated (1 min) and then filtered using a Costar Spin-X 0.45 μm cellulose acetate centrifuge tube filter (Corning, Corning, NY) prior to injection (100 μl, 0.5 mg protein) onto a PolyCATWAX 200 mm × 2.1 mm column with 5 μm (1000 Å) particles (PolyLC, Columbia, MD) using an Agilent 1200 series HPLC (Agilent Technologies, Palo Alto, CA) equipped with a binary pump, degasser, diode array detector and fraction collector. Mixed-bed weak cation/weak anion exchange (WCX/WAX or CATWAX) fractionation was performed at a flow rate of 200 μl/min using a gradient of 100% A held for 1 min, up to 8% B at 8 min, 85% B at 9.5 min, then 100% B at 12.5 min, and held at 100% B for an additional 17.5 min, where buffers A and B were 10 mM and 800 mM ammonium acetate in 20% acetonitrile (pH 7.2), respectively. The stand-alone weak cation exchange (WCX) and weak anion exchange (WAX) separations were performed on PolyCAT and PolyWAX 100 mm × 2.1 mm columns with 5 μm (1000 Å) particles (PolyLC, Columbia, MD), respectively. The WCX and WAX columns were also used in serial WCX-WAX and WAX-WCX configurations for dual-column weak cation/weak anion exchange experiments. In all cases, the UV absorbance was monitored at 220 and 280 nm. From the CATWAX separation, six fractions were collected over 22 min. The fractions were collected at the following intervals: 0–2, 2–4, 4–6, 6–14, 14–18 and 18–22 min, which were then evaporated to dryness under vacuum and kept at −30 °C prior to digestion.

2.4. Peptide fractionation

Protein digests were reconstituted in buffer A (120 μl, see below), sonicated (10 min), and centrifuged (5 min, 14,000 × *g*) prior to injection (100 μl, 0.5 mg protein) onto a Zorbax 300-SCX 150 mm × 2.1 mm column with 5 μm (300 Å) particles (Agilent Technologies, Palo Alto, CA) using the same HPLC system as for protein fractionation. SCX fractionation was performed at a flow rate of 250 μl/min with a gradient of 0–50% B in 15 min, up to 100% B at 25 min, then held for an additional 5 min at 100% B, where buffers A and B were 10 mM potassium dihydrogen phosphate in 25% acetonitrile (pH 2.75), and 1 M potassium chloride in buffer A (pH 2.75), respectively. UV absorbance was monitored at 220 and 280 nm. For trypsin samples, 3 min (0.75 ml) fractions were aliquoted into 1.5 ml tubes between 1.5 and 19.5 min, while for pepsin, 4 min (1.0 ml) fractions were collected between 1.5 and 25.5 min. Fractions were evaporated to dryness under vacuum and kept at −30 °C.

2.5. RP-UHPLC–MS/MS analysis

Dried samples were reconstituted in 10% acetonitrile (100 μl) and injected (20 μl) onto an Aeris PEPTIDE XB-C18 100 mm × 2.1 mm column, with solid core 1.7 μm particles (100 Å) (Phenomenex, Torrance, CA) on a Nexera UHPLC system (Shimadzu, Columbia, MD) with water (A) and acetonitrile (B), both containing 0.1% formic acid, at a flow rate of 300 μl/min (40 °C). The gradient started at 5% B, held for 2 min, and was increased linearly to 30% B at 24 min, to 50% B at 26 min, then to 85% B at 26.5 min. MS and MS/MS spectra were collected on a high-resolution TripleTOF 5600 mass spectrometer (AB Sciex, Concord, ON) equipped with a DuoSpray ion source in positive ion mode. The instrument performed a survey TOF-MS acquisition from *m/z* 140 to 1250 (250 ms accumulation time), followed by MS/MS on the 15 most intense precursor ions from *m/z* 250 to 1250 (excluded for 20 s after two occurrences) using information-dependent acquisition (IDA) with dynamic background subtraction. Each MS/MS acquisition had an accumulation time of 50 ms and collision energy of 30 ± 10 V. The total cycle time was 1.05 s.

2.6. Data treatment

MS/MS files from each workflow were combined and searched against the UniProt protein database (release date 26/06/2013) by ProteinPilot software (version 4.1) for the specified species (rat, mouse, or human) using Paragon algorithm [22], including false discovery rate (FDR) analysis and detection protein threshold of unused ProtScore > 0.05 (confidence > 10%). The search was performed for +2 to +4 charge states and MS tolerance was 0.05 Da on precursor ions and 0.1 Da on fragments. All duplicates were first processed alone, then together and finally tryptic and peptic digest for each sample were co-processed together. All strategies were then combined into a "master" file to represent the total number of proteins and peptides identified from all methods. Proteins were identified with a 1% global false discovery rate (FDR) using a target-decoy database search algorithm [23].

The list of UniProt accession numbers from identified proteins was uploaded to NCBI Batch Entrez to obtain the batch FASTA file, which was subsequently submitted to ExPASy for determination of isoelectric point and monoisotopic molecular weight and to Phobius [24] for prediction of IMPs, based on having at least one transmembrane domain (TMD ≥ 1). GRAVY Calculator was used to calculate grand average of hydropathy (GRAVY) scores. The list of accession numbers was also uploaded to PANTHER [25] for gene ontology (GO) classification. Venn diagrams were created by Venny interactive Venn diagram plotter (BioinfoGP) [26] while Clustal Omega [27] was used for multiple sequence alignment (MSA) analysis of the proteins unique to each dataset.

3. Results and discussions

Different sample fractionation methods were compared to achieve high proteome coverage for the analysis of rat liver microsomal (RLM) and S9 fractions (RLS). Several combinations of separation techniques including solid-phase

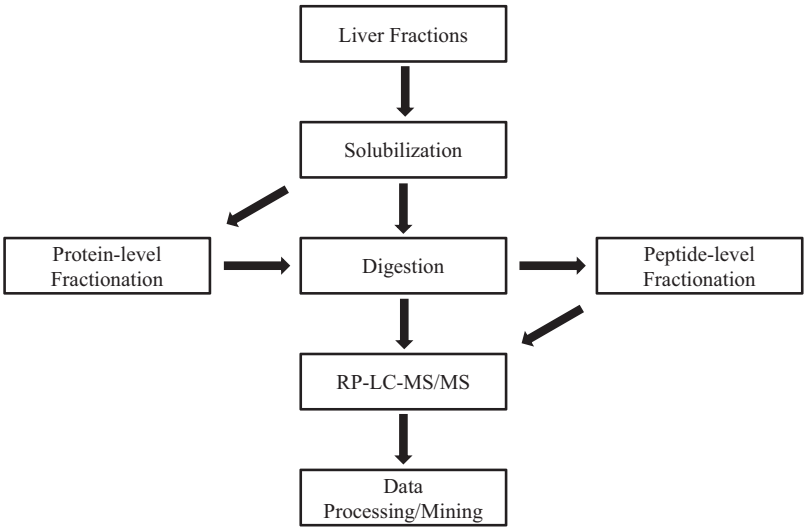

Fig. 1 – MDLC–MS/MS proteomic analysis workflow.

extraction (SPE), peptide-level ion exchange fractionation, and protein-level ion exchange fractionation were evaluated (Fig. 1). Each workflow was performed on pepsin and trypsin digested samples. The method with the best performance was then applied to the analysis of rat, mouse and human liver microsomal and S9 fractions. This cross-species comparison unveiled large overlaps between the datasets obtained and further analysis of the results shed light on possible orthologs between the species.

3.1. *Method optimization*

For protein solubilization, SDS is often used, however, it is known to cause technical difficulties, interfering with downstream MS analysis, thus needs to be effectively removed prior to LC–MS [28]. In previous work, SDS-assisted tryptic digestion yielded better results than several other solubilizing agents when peptide-level ion exchange fractionation was performed prior to LC–MS analysis [18]. The current study also tested the effect of SDS on pepsin digestion efficiency with and without detergent removal by TCA precipitation. The SDS-solubilized peptic digestion without TCA precipitation yielded the highest number of identified proteins at a 1% final SDS concentration (in 0.1% TFA, 10% methanol) (data not shown). During the SPE clean-up step, different elution conditions were tested on peptic digests (from RLM and RLS) using OASIS HLB cartridges (Waters, Milford, MA). Elution with 100% methanol yielded the highest number of identified peptides and proteins at 1% FDR, followed by a 60:40 mixture of ACN/isopropanol, and 100% ACN exhibited the least favorable results (unpublished data).

For LC–MS/MS acquisition, elution gradients and MS/MS parameters were assessed for the analysis of RLM digests (after SPE clean-up). The LC method employed in previous work [18] was further optimized by varying flow rates and gradient conditions slightly, with the goal of keeping a reasonable throughput (30–40 min per run). A flow rate of 300 μl/min offered better separation efficiency compared to 250 and 350 μl/min using the solid-core 1.7 μm C18 column. Based on the total ion chromatogram (TIC) of the TOF-MS survey scan; the gradient was modified to 5% B held for 2 min, gradually increased to 30% B at 24 min, to 50% B at 26 min, then to 85% B at 26.5 min and held for 2 min. These LC conditions yielded extremely reproducible retention times between samples over the course of this study. In terms of IDA criteria, the maximum number of candidate ions for the MS/MS dependent scans per cycle was varied between 5 and 20 ions with an accumulation time ranging from 50 to 200 ms for each MS/MS. The intensity threshold of the IDA candidate ions was also varied from 200 to 500 cps and isotope exclusion was tested at 2 or 3 Da. Moreover, MS/MS acquisition of the precursor ion was excluded after two MS/MS scans for either 15, 20 or 30 s. Optimization of the IDA-MS/MS parameters resulted in 15 MS/MS with 50 ms accumulation time each, a 3 Da isotope exclusion and 20 s dynamic exclusion for selected precursor ions. This led to a significant improvement of the number of identified peptides, proteins and IMPs as well as higher average protein sequence % coverage and shorter total cycle time (summarized in Table 1). A more detailed comparison can be found in Supplemental Table S1.

3.2. *2D-LC–MS/MS using protein-level fractionation*

For protein pre-fractionation of microsomal and S9 fractions, five workflows were examined in this study, incorporating WCX and WAX in different combinations. Single WCX and WAX runs were compared to tandem WCX-WAX and WAX-WCX using two columns in series, as well as mixed-bed WCX/WAX (CATWAX) using identical gradient conditions. Judging by the LC–UV traces, single ion-exchange did not yield satisfactory separations, though WAX did perform better than WCX. Tandem combinations of WCX-WAX and WAX-WCX improved the separation, although CATWAX provided more resolution due to the potential of retaining both negatively and positively charged proteins over the single column in a homogeneous manner (Supplemental Figure S1).

Table 1 – Improvements achieved by optimization of the IDA–MS/MS parameters.

	Initial conditions[a]	Optimized conditions[b]	Δ
# Peptides (1% FDR)	7570	17,566	132%
# Proteins (1% FDR)	768	1120	46%
Avg. seq. % coverage	25.0	29.9	20%
# IMP	147	217	48%
Acquisition speed	1.30 s/cycle	1.05 s/cycle	−19%

[a] 10 MS/MS scans (100 ms accumulation time) without dynamic exclusion.
[b] 15 MS/MS scans (50 ms accumulation time) with 20 s dynamic exclusion.

3.3. 2D-LC–MS/MS using peptide-level fractionation

LC–UV traces from SCX fractionation of the microsomal and S9 digested samples demonstrated a separation pattern similar to that of the protein-level fractionation (two elution zones). Tryptic digests gave a more significant UV absorption in the second portion than the earlier elution zone at 2–5 min, compared to pepsin, which seemed to have a wider elution profile overall. This is attributed to the tendency of trypsin to cleave after lysine and arginine residues resulting in more basic peptides strongly binding to the aromatic sulfonic acid groups of the SCX column. The wider spread of elution for peptic digests was attributed to more variety possible in terms of basicity as pepsin cuts at non-charged (hydrophobic) amino acids (Fig. 2).

Previous work using 2D(SCX-RP)-LC–MS/MS for rat liver microsomes [18] incorporated a protein precipitation step prior to digestion to remove membrane-associated impurities as well as excess reagents which may hinder digestion or affect SCX separation efficiency [29]. This precipitation step was replaced by a SPE clean-up step prior to SCX fractionation, to achieve good separation efficiency.

3.4. 3D-LC–MS/MS (combined protein- and peptide-level fractionation)

LC–MS/MS analysis with multiple dimensions of pre-fractionation has proven useful in proteomics research [2], with reports of improved protein/peptide identification [30–32], higher peptide selectivity [33] and more efficient detection of modifications [34,35]. However, most of these have combined successive LC steps at the peptide level. In this study, the 3D-LC–MS/MS approach tested combined protein-level (CATWAX) with dual peptide-level (SCX-RP) separations. Unfortunately, the results showed poor performance compared to both regular 1D-(RP) and the 2D-(SCX-RP) methods. All protein-level fractions, when subjected to peptide fractionation, yielded identical chromatographic traces. Several sample treatment workflows were tested incorporating SDS-assisted solubilization or acetone/TCA protein precipitation, however, no significant improvement was observed.

3.5. Tryptic versus peptic digestion

A parallel tryptic–peptic dual digestion was performed for the analysis of rat liver microsomes for increased proteome coverage due to the complementary cleavage sites between the two enzymes [18]. Trypsin normally cleaves at basic amino acid residues such as arginine and lysine which are more abundant in water-soluble proteins. Pepsin, on the other hand, targets residues with hydrophobic and preferably aromatic side chains such as leucine, phenylalanine, tryptophan, and tyrosine [36], likely found in less water-soluble regions, such as membrane proteins. Microsomes (and S9 fractions) are rich sources of membrane proteins and therefore a combined tryptic–peptic digestion enhances the proteome coverage as pepsin cleaves regions embedded inside (or associated with) the membrane while trypsin cuts more solvent-exposed regions. Table 2 summarizes the results obtained from trypsin and pepsin digestions using four fractionation strategies. As expected, trypsin led to a higher number of identified proteins and peptides, while pepsin often yielded an increased %IMP. Moreover, replicate analysis showed that, overall, trypsin samples had better reproducibility compared to pepsin samples (see Supplemental Table S2). It was also observed that 23–51% of the identified proteins were shared between trypsin and pepsin, 37–72% were unique to trypsin, and 4–12% were unique to peptic digestion. The pepsin-unique proteins included more IMPs (up to 40%) compared to trypsin-specific proteins (up to 20%). More details on the overlap analysis can be found in Supplemental Table S3.

3.6. Comparison of the four workflows

The results from 1D-, 2D- and 3D-LC–MS/MS approaches showed significantly superior performance of the 2D-(SCX-RP) workflow. Based on previous research [9,10], it was expected that the best performance would be seen with the 3D strategy, combining fractionation at both protein and peptide levels. Nevertheless, the 2D-(CATWAX-RP) and 3D-(CATWAX-SCX-RP) methods led to less satisfactory results even compared to the regular 1D-RP (Table 2). This is most likely related to sample loss related to protein fractionation. Proteins identified exclusively with sample preparation workflows involving protein fractionation were compared between RLM (94 proteins) and RLS (86 proteins). What was seen is that most (90%) of these 154 proteins (RLM + RLS, non-redundant) have negative GRAVY scores; hence they are more water soluble. This is in line with the assumption that recovery problems from protein fractionation workflows were caused by solubility issues. Separating complex mixtures of proteins is challenging, especially for samples containing membrane proteins such as liver microsomes/S9 fractions.

Using the 2D-SCX-RP method (combining trypsin + pepsin digestion results), 17,566 distinct peptides were detected

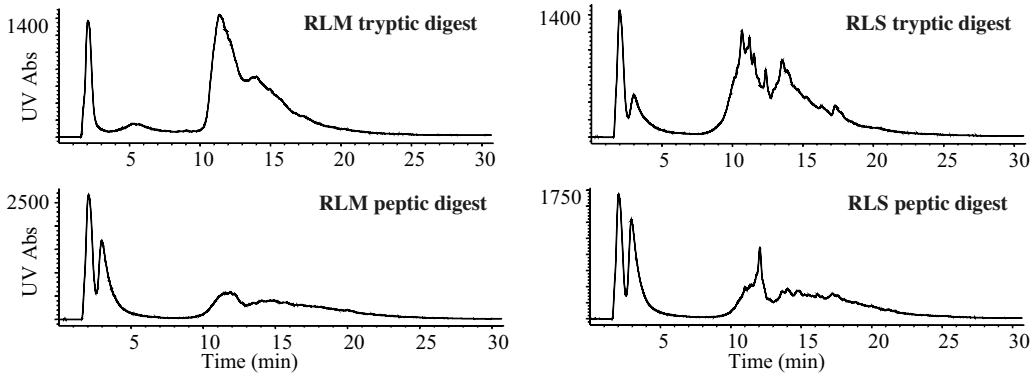

Fig. 2 – LC–UV traces at 220 nm from the SCX peptide-level fractionation of RLM (left) and RLS (right) samples digested by trypsin (top) or pepsin (bottom).

(1% FDR) in RLM leading to 1120 identified proteins (1% FDR), with ~30% average protein sequence coverage, out of which 212 proteins (19%) were predicted to be transmembrane proteins (based on analysis using Phobius). From RLS samples, 15,905 distinct peptides and 1037 proteins were found with 28% protein sequence coverage. The S9 fractions also contained less transmembrane proteins (102, equivalent to 10%), which was anticipated, since both cytosolic and microsomal proteins are present [37]. Both sample types yielded the same ranking of performance between 1D, 2D-CATWAX-RP and 3D workflows (Table 2). The 2D-SCX-RP approach provided the highest number of unique proteins (486 in RLM, 440 in RLS). A total number of 170 in RLM and 96 in RLS were common to all four workflows (Fig. 3). Moreover, if average sequence coverage is compared for these shared proteins, the SCX-RP method was again superior (61% vs 43% for 1D, 22% for CATWAX-RP, and 23% for 3D).

3.7. *Rat proteome results*

The rat liver proteome has been widely studied with the aim of improving existing knowledge on this specialized tissue. Several recent studies were performed to address questions in pathogenesis and development of liver cancer and chronic

Table 2 – Comparative results from the analysis of rat liver microsomes (RLM) and S9 fractions (RLS) using the four fractionation approaches (trypsin, pepsin, and the two enzymes combined).

Sample[a]	Approach	Digestion	Proteins[b]	Peptides[b]	Avg. sequence coverage (%)	IMP (%IMP)[c]
RLM	1D	Trypsin	543	4643	22.2	96 (17.7)
		Pepsin	390	2453	16.0	90 (23.1)
		Combined	586	7049	27.1	107 (18.3)
	CATWAX	Trypsin	286	1384	16.1	23 (8.0)
		Pepsin	138	848	20.6	7 (5.1)
		Combined	297	2188	19.8	20 (6.7)
	SCX	Trypsin	1089	12,111	24.8	217 (19.9)
		Pepsin	610	5251	20.9	134 (22.0)
		Combined	1120	17,566	29.9	212 (18.9)
	3D	Trypsin	365	1493	15.0	39 (10.7)
		Pepsin	177	737	13.5	20 (11.3)
		Combined	370	2109	16.8	45 (12.2)
RLS	1D	Trypsin	521	4721	22.1	51 (9.8)
		Pepsin	320	1817	13.4	33 (10.3)
		Combined	569	6497	24.0	52 (9.1)
	CATWAX	Trypsin	253	1190	17.8	13 (5.1)
		Pepsin	74	541	24.1	2 (2.7)
		Combined	260	1707	20.1	10 (3.8)
	SCX	Trypsin	1015	11,453	25.0	101 (10.0)
		Pepsin	502	4291	18.4	51 (10.2)
		Combined	1037	15,905	28.4	102 (9.8)
	3D	Trypsin	175	676	14.4	15 (8.0)
		Pepsin	67	325	17.5	4 (6.0)
		Combined	174	975	15.8	14 (8.0)

[a] Data combined from duplicate samples.
[b] Total number of proteins/peptides identified (from duplicate samples) with 1% FDR.
[c] Percentage of integral membrane proteins identified for each condition.

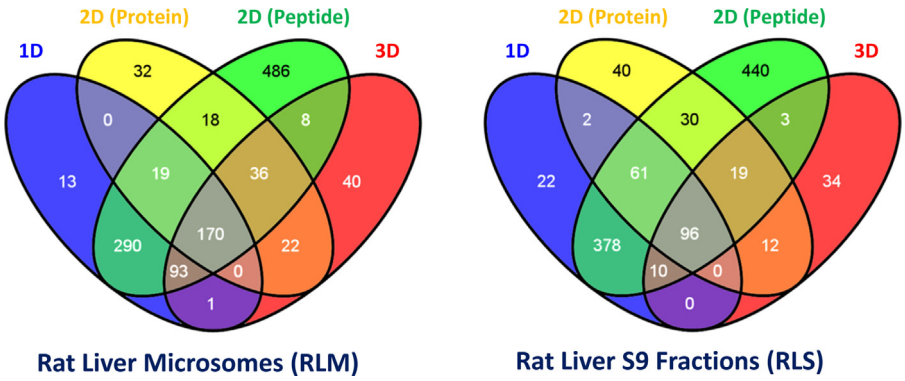

Fig. 3 – Venn diagrams representing the number of identified proteins in RLM (left) and RLS (right) using 1D-, 2D- and 3D-LC–MS/MS workflows.

diseases [38–40], drug evaluation [41] and drug-induced liver injury [42–45], and understanding of cellular functions [46–48]. Most recently, in an extensive study on whole rat liver homogenate, using an integrated "*omics*" approach on two rat strains (BN-Lx and SHR) combining multiple proteases (trypsin, Lys-C, Glu-C, Asp-N, and chymotrypsin), SCX fractionation and LC-MS/MS analysis on two platforms (TripleTOF 5600 and LTQ-Orbitrap Velos), Low et al. obtained peptide evidence for 26,463 proteins with an overall sequence coverage of 15.6% [38]. This impressive result was obtained based on searching a custom-built database with the goal of achieving a complete inventory of genetic variation, combining data from genome and RNA sequencing, which includes genetic polymorphisms and post-transcriptional events. For comparative purposes, the analysis presented here was performed on Sprague-Dawley rat liver fractions with two proteases and one MS/MS platform, using the UniProt KB/Swiss-Prot database, comprising total of 7887 reviewed protein entries.

The current study incorporated a total of 491,615 (RLM) and 426,812 (RLS) high-resolution MS/MS spectra from the four strategies leading to the identification of 1185 (RLM) and 1081 (RLS) proteins at 1% FDR, of which 796 proteins (54%) were common between the two datasets, while 674 proteins (46%) were unique to either microsomes or S9 fraction. Combining the two datasets and removing redundancies, a total number of 1400 proteins were identified in the studied rat liver fractions, of which 1235 (88.2%) were also reported by Low et al. [38].

Using Phobius (combined transmembrane topology and signal peptide predictor) [24], 215 and 103 IMPs was found in RLM (18% identified proteins) and RLS (10% identified proteins), respectively. An average of 5 and 7 peptides (confidence >95%) were detected for each protein in RLM and RLS, respectively. However, the average protein sequence coverage was similar between RLM (31.4%) and RLS (29.9%) samples. Sequence coverage is of particular importance for studies involving protein modifications, since the higher the coverage, the better the chances of detecting covalent modifications on a target protein. Our group is particularly interested in elucidating novel protein targets of reactive molecules and therefore this was set as a high priority when optimizing the proteomic analysis workflow.

Characterizing the overall distribution of p*I*, molecular weights, and GRAVY scores is of interest when optimizing sample preparation steps (ion exchange, SPE, etc.) for increasing coverage of the proteomic analysis. Therefore, an in-depth analysis of the identified proteins was performed on the rat liver samples. From the compiled dataset, RLM and RLS proteins were analyzed in terms of their physicochemical properties. A comparison of protein p*I* revealed that the majority of rat liver proteins have a theoretical p*I* in the range of 4–12 with 43.4% (RLM) and 34.8% (RLS) with basic characteristics (p*I* > 7). Considering the MW distribution, 2–3% of proteins were below 10 kDa, 60–62% in the range from 10 to 50 kDa, 29–30% in the range from 50 to 100 kDa, and 6–7% above 100 kDa, with an average molecular mass of 48.2 and 50.1 kDa for RLM and RLS, respectively. The identified proteins were also analyzed in terms of hydropathy (as measured by GRAVY scores). With a GRAVY score distribution in the range from −2.0 to 1.1, 16.8% of RLM and 12.9% of RLS proteins were characterized as hydrophobic (GRAVY < 0), coinciding well with the %IMPs predicted by Phobius (Fig. 4). The identified proteins in rat liver samples were also analyzed in terms of biological properties using PANTHER [25]. As depicted in Fig. 5, GO analysis classified RLM and RLS proteins into 10 groups based on their molecular functions, over 45% of which represent catalytic functions. Interestingly, there were more transporter and receptor proteins identified in the microsomes than in the S9 fraction whereas the latter sample was richer in structural, molecule-binding, translation and enzyme regulator proteins. When classified by biological processes, 12 groups were identified with the highest proportion being involved in metabolic and cellular processes. However, it was seen that a slightly higher proportion of the microsomal proteins were involved in localization and multicellular organismal processes, while more proteins were associated with biological regulation, cellular, developmental and metabolic processes from the S9 fraction. Many of these proteins play a crucial role in the metabolism of xenobiotics and thus are interesting for toxicology and drug discovery studies.

3.8. *Cross-species comparison of liver proteins*

Rat and mouse are common animal models for various applications related to human metabolism, pharmacology

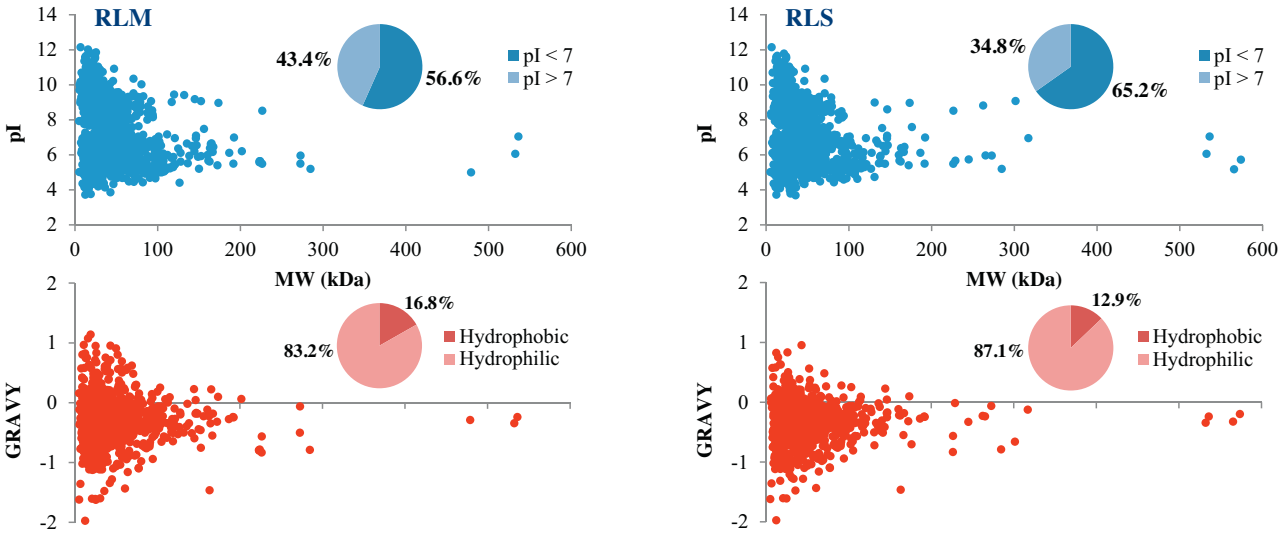

Fig. 4 – Statistical distribution of isoelectric point (above) and GRAVY score (below) as a function of MW for the proteins identified in RLM (right) and RLS (left).

and toxicology. Cross-species studies are informative for extrapolation of these models to humans [49]. Cross-species proteomics can also contribute to characterizing proteins of unknown function, especially between closely related species which often have important sequence similarities [50]. Using the workflow optimized for the analysis of rat samples, mouse and human liver fractions were also analyzed and the datasets were compared. Table 3 summarizes the results from the analysis of microsomal and S9 fractions of all three species. Overall, 1400 distinct proteins were identified at 1% FDR in rat, 1791 in mouse, and 1939 in human with an average sequence coverage of 23–30%, an average of 8–10 peptides (confidence > 95%) per protein, and a reproducibility of 62–80% (for separately fractionated duplicate samples). Also, similar to

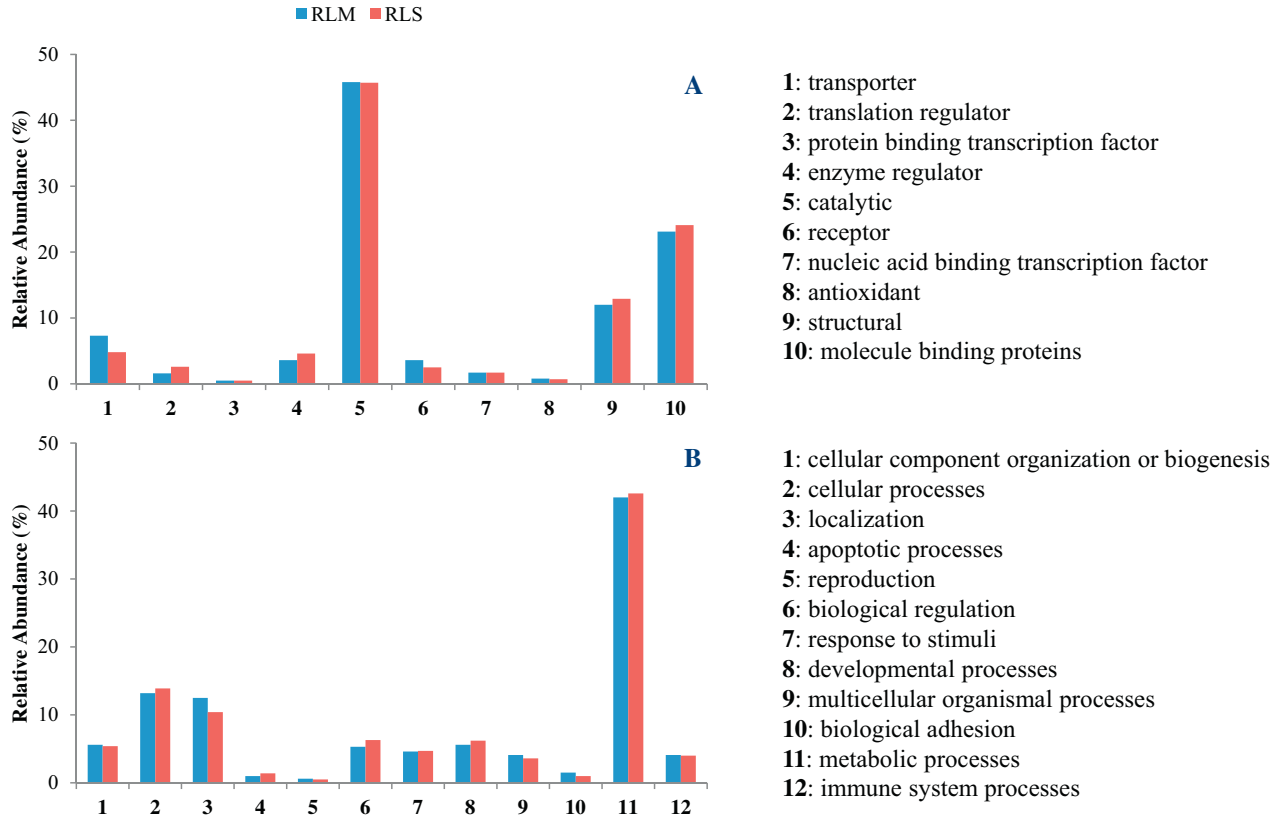

Fig. 5 – Gene ontology annotations based on molecular function (A) and biological process (B) for the proteins identified in RLM and RLS.

Table 3 – Proteomic analysis of rat, mouse and human liver microsomes and S9 fractions using the optimized 2D-LC–MS/MS method.

Species	Sample	Proteins[a]	Peptides[a]	IMP (%)	Sequence % coverage[b]	Peptides per protein[b]	Total proteins[a]
Rattus norvegicus	Microsomes	1120	17,566	217 (19.4)	29.9	10	1400
	S9 fraction	1037	15,905	104 (10.0)	28.4	10	
Mus musculus	Microsomes	1582	19,262	294 (18.6)	24.9	8	1791
	S9 fraction	1538	18,089	271 (17.6)	22.9	8	
Homo sapiens	Microsomes	1516	18,739	308 (20.3)	24.0	8	1939
	S9 fraction	1570	20,435	188 (12.0)	24.2	8	

[a] Number of proteins and peptides at 1% FDR
[b] Average of all identified proteins

rat, microsomes contained a higher number of IMPs than S9 fractions in both mouse and human. As expected, the proteins identified in the three species demonstrated a high amount of similarity in terms of both physicochemical and biological properties, as illustrated in Supplemental Figures S2-S3. As for isoelectric points, 38.6–43.1% of the proteins have p*I* > 7, whereas 15.6–16.4% could be classified as hydrophobic, coinciding well with the number of IMPs in each sample. Moreover, GO classification revealed that rat, mouse and human liver proteins are analogous in terms of function and involvement in biological processes, as expected.

As shown in Fig. 6, when a cross-species analysis was performed, comparing gene IDs only, on all datasets, 31.3% and 28.0% orthologous proteins were found between the three species for microsomal and S9 fractions, respectively, while approximately 44% were deemed as unique to one species. The combined results from microsomal and S9 fractions are shown in Supplemental Figure S4. MSA analysis, performed

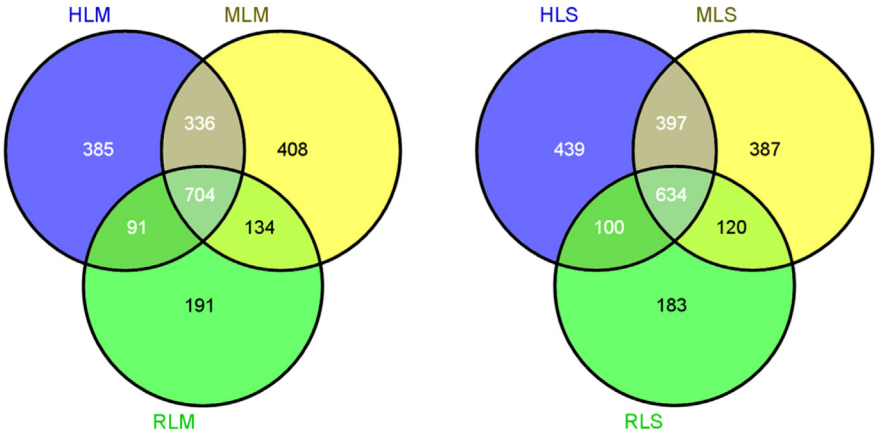

Fig. 6 – Venn diagrams depicting the number of shared and unique proteins identified in rat, mouse and human liver microsomal (left) and liver S9 (right) proteins.

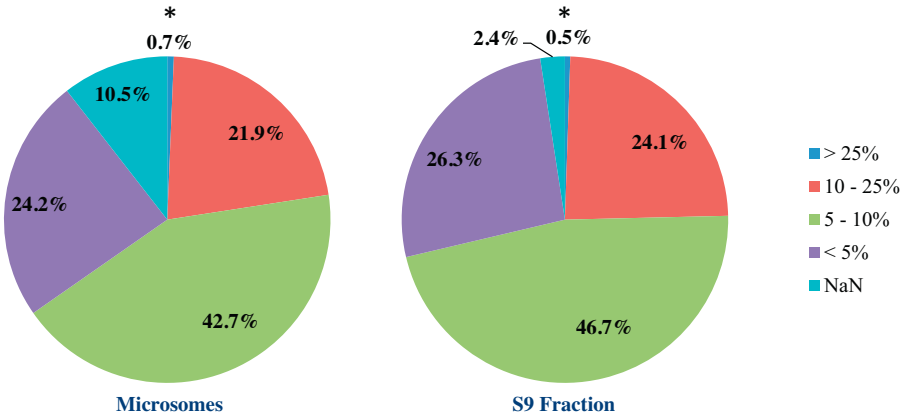

Fig. 7 – Percent alignment of proteins unique to rat, mouse or human liver microsomes (left) or S9 fraction (right). Labels (from the legend on right) are distributed in the pie charts from the * in a clockwise manner (The term NaN stands for "not a number").

to assess the non-orthologous proteins, demonstrated that for 22.6% (microsomal) and 24.6% (S9) of these proteins had reasonable sequence similarities, with at least 10% inter-species homology (Fig. 7). Taking into consideration all the identified proteins (microsomal and S9), MSA analysis revealed that the set of human proteins are slightly more homologous to rat than mouse (Supplemental Figure S5). Percent identity matrices (PIMs) and phylogenetic trees from this analysis are available in Supplemental Table S4.

A complete list of the proteins identified (at 1% FDR) in each sample, and the distinct peptides detected for each protein is published as a *Data in Brief* article [51]. In this related article, links to publicly accessible repositories are provided. In an effort to quantify the impact of making this data publicly available, the lists of peptides from tryptic digestion of human, mouse and rat samples were compared to the most recent database entries on PeptideAtlas (2013-11, 2014-12 and 2014-08 builds for rat, mouse and human, respectively) [52]. Remarkably, a relatively large proportion of our highly confident peptides were not found in the most current version of PeptideAtlas (20.1% of the human peptides, and 35.8% for each of the mouse and rat peptide lists). Therefore, once incorporated, this large dataset would add a significant amount of additional information into this publicly accessible database. These data would be useful for subsequent studies involving quantitative proteomics applications as well as further probing of biological information contained in these rich datasets.

Liver microsomes and S9 fractions are routinely used in drug metabolism studies and therefore, an in-depth characterization of the proteins contained in these fractions is of particular interest for probing protein modifications resulting via drug bioactivation (reactive metabolites). Several studies have been performed with the goal of identifying protein targets of reactive compounds in liver microsomes [53–56], and we anticipate this comprehensive proteomic analysis of these three species will facilitate future work in this challenging area.

4. Conclusion

Sample preparation and enrichment is a crucial step in the analysis of complex samples and directly affects the efficiency of any proteomic workflow. In this study, a parallel dual digestion method followed by a comparison of different fractionation strategies prior to UHPLC–MS/MS was employed in the analysis of rat liver microsomal and S9 fractions.

Protein-level fractionation using mixed-bed weak cation/anion exchange (CATWAX) did not improve proteome coverage for these samples, compared to the 1D(RP)-LC–MS/MS workflow and did not ameliorate results when combined with peptide-level SCX fractionation either. The 2D(SCX-RP)-LC–MS/MS approach yielded the best results and was therefore chosen for the comparative analysis of rat, mouse and human liver fractions.

Informative results including physicochemical properties and GO classification of the identified proteins, as well as an overall comparison of homology between the three species was performed.

This study resulted in large sets of high-resolution MS/MS data yielding impressive proteome coverage for challenging liver fractions containing a relatively high number of membrane proteins. The results of this work are of particular interest to the drug discovery and toxicology communities. This information could be specifically useful in several applications, for example cross-species extrapolation of toxicity, characterizing protein modifications, and developing targeted quantitative assays for verification of potential biomarker panels.

Conflict of interest

The authors declare no conflict of interest pertaining to the publication of this manuscript.

Funding sources

Financial support for this study was provided by the Natural Sciences and Engineering Research Council of Canada (Discovery Grant no. 355933-2011).

Acknowledgements

M. G. would like to thank GRASP (*Groupe de Recherche Axé sur la Structure des Protéines*, FRSQ) and *la Fondation de l'UQÀM* (*Bourses d'Excellence des Cycles Supérieurs* FARE) scholarships. Authors would also like to thank Dr. Sean Seymour (AB Sciex), Dr. Eric Deutsch (Institute for System Biology/PeptideAtlas) and the PRIDE team for their kind and timely support.

Appendix A. Supplementary data

Supplementary data associated with this article can be found, in the online version, at doi:10.1016/j.euprot.2015.01.003.

REFERENCES

[1] Holčapek M, Jirásko R, Lísa M. Recent developments in liquid chromatography–mass spectrometry and related techniques. J Chromatogr A 2012;1259:3–15, http://dx.doi.org/10.1016/j.chroma.2012.08.072.
[2] Wu Q, Yuan H, Zhang L, Zhang Y. Recent advances on multidimensional liquid chromatography–mass spectrometry for proteomics: from qualitative to quantitative analysis – a review. Anal Chim Acta 2012;731:1–10, http://dx.doi.org/10.1016/j.aca.2012.04.010.
[3] Xie F, Smith RD, Shen Y. Advanced proteomic liquid chromatography. J Chromatogr A 2012;1261:78–90, http://dx.doi.org/10.1016/j.chroma.2012.06.098.
[4] Di Palma S, Hennrich ML, Heck AJR, Mohammed S. Recent advances in peptide separation by multidimensional liquid chromatography for proteome analysis. J Proteomics 2012;75:3791–813, http://dx.doi.org/10.1016/j.jprot.2012.04.033.
[5] Nice EC, Rothacker J, Weinstock J, Lim L, Catimel B. Use of multidimensional separation protocols for the purification of trace components in complex biological samples for

proteomics analysis. J Chromatogr A 2007;1168:190–210, http://dx.doi.org/10.1016/j.chroma.2007.06.015.
[6] Gilar M, Olivova P, Daly AE, Gebler JC. Orthogonality of separation in two-dimensional liquid chromatography. Anal Chem 2005;77:6426–34, http://dx.doi.org/10.1021/ac050923i.
[7] Peng J, Elias JE, Thoreen CC, Licklider LJ, Gygi SP. Evaluation of multidimensional chromatography coupled with tandem mass spectrometry (LC/LC–MS/MS) for large-scale protein analysis: the yeast proteome. J Proteome Res 2003;2:43–50, http://dx.doi.org/10.1021/pr025556v.
[8] Havugimana PC, Wong P, Emili A. Improved proteomic discovery by sample pre-fractionation using dual-column ion-exchange high performance liquid chromatography. J Chromatogr B 2007;847:54–61, http://dx.doi.org/10.1016/j.jchromb.2006.10.075.
[9] Motoyama A, Xu T, Ruse CI, Wohlschlegel JA, Yates JR. Anion and cation mixed-bed ion exchange for enhanced multidimensional separations of peptides and phosphopeptides. Anal Chem 2007;79:3623–34, http://dx.doi.org/10.1021/ac062292d.
[10] Zhang L, Yao L, Zhang Y, Xue T, Dai G, Chen K, et al. Protein pre-fractionation with a mixed-bed ion exchange column in 3D LC–MS/MS proteome analysis. J Chromatogr B 2012;905:96–104, http://dx.doi.org/10.1016/j.jchromb.2012.08.008.
[11] Van Summeren A, Renes J, van Delft JHM, Kleinjans JCS, Mariman ECM. Proteomics in the search for mechanisms and biomarkers of drug-induced hepatotoxicity. Toxicol In Vitro 2012;26:373–85, http://dx.doi.org/10.1016/j.tiv.2012.01.012.
[12] Mathias RA, Chen Y-S, Kapp EA, Greening DW, Mathivanan S, Simpson RJ. Triton X-114 phase separation in the isolation and purification of mouse liver microsomal membrane proteins. Methods 2011;54:396–406, http://dx.doi.org/10.1016/j.ymeth.2011.01.006.
[13] Imming P, Sinning C, Meyer A. Drugs, their targets and the nature and number of drug targets. Nat Rev Drug Discov 2006;5:821–34, http://dx.doi.org/10.1038/nrd2132.
[14] Helbig AO, Heck AJR, Slijper M. Exploring the membrane proteome – challenges and analytical strategies. J Proteomics 2010;73:868–78, http://dx.doi.org/10.1016/j.jprot.2010.01.005.
[15] Gilmore JM, Washburn MP. Advances in shotgun proteomics and the analysis of membrane proteomes. J Proteomics 2010;73:2078–91, http://dx.doi.org/10.1016/j.jprot.2010.08.005.
[16] Plant N. Strategies for using in vitro screens in drug metabolism. Drug Discov Today 2004;9:328–36.
[17] Zhou S, Chan E, Duan W, Huang M, Chen Y-Z. Drug bioactivation, covalent binding to target proteins and toxicity relevance. Drug Metab Rev 2005;37:41–213, http://dx.doi.org/10.1081/DMR-200028812.
[18] Golizeh M, Sleno L. Optimized proteomic analysis of rat liver microsomes using dual enzyme digestion with 2D-LC–MS/MS. J Proteomics 2013;82:166–78, http://dx.doi.org/10.1016/j.jprot.2013.02.001.
[19] Langenfeld E, Zanger UM, Jung K, Meyer HE, Marcus K. Mass spectrometry-based absolute quantification of microsomal cytochrome P450 2D6 in human liver. Proteomics 2009;9:2313–23, http://dx.doi.org/10.1002/pmic.200800680.
[20] Bucher J, Riedmaier S, Schnabel A, Marcus K, Vacun G, Weiss TS, et al. A systems biology approach to dynamic modeling and inter-subject variability of statin pharmacokinetics in human hepatocytes. BMC Syst Biol 2011;5:66, http://dx.doi.org/10.1186/1752-0509-5-66.
[21] Schaefer O, Ohtsuki S, Kawakami H, Inoue T, Liehner S, Saito A, et al. Absolute quantification and differential expression of drug transporters, cytochrome P450 enzymes, and UDP-glucuronosyltransferases in cultured primary human hepatocytes. Drug Metab Dispos 2012;40:93–103, http://dx.doi.org/10.1124/dmd.111.042275.
[22] Shilov IV, Seymour SL, Patel AA, Loboda A, Tang WH, Keating SP, et al. The Paragon Algorithm, a next generation search engine that uses sequence temperature values and feature probabilities to identify peptides from tandem mass spectra. Mol Cell Proteomics 2007;6:1638–55, http://dx.doi.org/10.1074/mcp.T600050-MCP200.
[23] Tang WH, Shilov IV, Seymour SL. Nonlinear fitting method for determining local false discovery rates from decoy database searches. J Proteome Res 2008;7:3661–7, http://dx.doi.org/10.1021/pr070492f.
[24] Krogh A, Sonnhammer ELL, Käll L. Advantages of combined transmembrane topology and signal peptide prediction—the Phobius web server. Nucleic Acids Res 2007;35:429–32, http://dx.doi.org/10.1093/nar/gkm256.
[25] Thomas PD, Kejariwal A, Campbell MJ, Mi H, Diemer K, Guo N, et al. PANTHER: a browsable database of gene products organized by biological function, using curated protein family and subfamily classification. Nucleic Acids Res 2003;31:334–41, http://dx.doi.org/10.1093/nar/gkg115.
[26] Oliveros JC. VENNY. An interactive tool for comparing lists with Venn diagrams; 2007. http://bioinfogp.cnb.csic.es/tools/venny/index.html
[27] Sievers F, Wilm A, Dineen D, Gibson TJ, Karplus K, Li W, et al. Fast, scalable generation of high-quality protein multiple sequence alignments using Clustal Omega. Mol Syst Biol 2011;7:539, http://dx.doi.org/10.1038/msb.2011.75.
[28] Griffin NM, Schnitzer JE. Overcoming key technological challenges in using mass spectrometry for mapping cell surfaces in tissues. Mol Cell Proteomics 2011;10, http://dx.doi.org/10.1074/mcp.R110.000935.
[29] Westermeier R, Naven T. Proteomics in practice – a laboratory manual of proteome analysis. Weinheim, Germany: Wiley-VCH; 2002.
[30] Boichenko AP, Govorukhina N, van der Zee AGJ, Bischoff R. Multidimensional separation of tryptic peptides from human serum proteins using reversed-phase, strong cation exchange, weak anion exchange, and fused-core fluorinated stationary phases. J Sep Sci 2013;36:3463–70, http://dx.doi.org/10.1002/jssc.201300750.
[31] Li Q, Jain MR, Chen W, Li H. A multidimensional approach to an in-depth proteomics analysis of transcriptional regulators in neuroblastoma cells. J Neurosci Methods 2013;216:118–27, http://dx.doi.org/10.1016/j.jneumeth.2013.03.016.
[32] Rodríguez AA, Ständker L, Zaharenko AJ, Garateix AG, Forssmann W-G, Béress L, et al. Combining multidimensional liquid chromatography and MALDI-TOF-MS for the fingerprint analysis of secreted peptides from the unexplored sea anemone species *Phymanthus crucifer*. J Chromatogr B 2012;903:30–9, http://dx.doi.org/10.1016/j.jchromb.2012.06.034.
[33] Betancourt LH, De Bock P-J, Staes A, Timmerman E, Perez-Riverol Y, Sanchez A, et al. SCX charge state selective separation of tryptic peptides combined with 2D-RP-HPLC allows for detailed proteome mapping. J Proteomics 2013;91:164–71, http://dx.doi.org/10.1016/j.jprot.2013.06.033.
[34] McClintock CS, Parks JM, Bern M, Ghattyvenkatakrishna PK, Hettich RL. Comparative informatics analysis to evaluate site-specific protein oxidation in multidimensional LC–MS/MS data. J Proteome Res 2013;12:3307–16, http://dx.doi.org/10.1021/pr400141p.
[35] Tousi F, Bones J, Iliopoulos O, Hancock WS, Hincapie M. Multidimensional liquid chromatography platform for profiling alterations of clusterin N-glycosylation in the plasma of patients with renal cell carcinoma. J Chromatogr

A 2012;1256:121–8, http://dx.doi.org/10.1016/j.chroma.2012.07.066.
[36] Dunn BM. Structure and mechanism of the pepsin-like family of aspartic peptidases. Chem Rev 2002;102:4431–58, http://dx.doi.org/10.1021/cr010167q.
[37] Duffus JH, Nordberg M, Templeton DM. Glossary of terms used in toxicology, 2nd edition (IUPAC recommendations 2007). Pure Appl Chem 2007;79:1153–344, http://dx.doi.org/10.1351/pac200779071153.
[38] Low TY, van Heesch S, van den Toorn H, Giansanti P, Cristobal A, Toonen P, et al. Quantitative and qualitative proteome characteristics extracted from in-depth integrated genomics and proteomics analysis. Cell Rep 2013;5:1469–78, http://dx.doi.org/10.1016/j.celrep.2013.10.041.
[39] Hu X, Duan Z, Hu H, Li G, Yan S, Wu J, et al. Proteomic profile of carbonylated proteins in rat liver: exercise attenuated oxidative stress may be involved in fatty liver improvement. Proteomics 2013;13:1755–64, http://dx.doi.org/10.1002/pmic.201200522.
[40] Cao L, Clifton JG, Reutter W, Josic D. Mass spectrometry-based analysis of rat liver and hepatocellular carcinoma Morris hepatoma 7777 plasma membrane proteome. Anal Chem 2013;85:8112–20, http://dx.doi.org/10.1021/ac400774g.
[41] Wang X, Zhang A, Wang P, Sun H, Wu G, Sun W, et al. Metabolomics coupled with proteomics advancing drug discovery toward more agile development of targeted combination therapies. Mol Cell Proteomics 2013;12:1226–38, http://dx.doi.org/10.1074/mcp.M112.021683.
[42] Van Swelm RPL, Hadi M, Laarakkers CMM, Masereeuw R, Groothuis GMM, Russel FGM. Proteomic profiling in incubation medium of mouse, rat and human precision-cut liver slices for biomarker detection regarding acute drug-induced liver injury. J Appl Toxicol 2014;34:993–1001, http://dx.doi.org/10.1002/jat.2917.
[43] Zhang H, Hou J, Cui R, Guo X, Shi Z, Yang F, et al. Phosphoproteome analysis reveals an important role for glycogen synthase kinase-3 in perfluorododecanoic acid-induced rat liver toxicity. Toxicol Lett 2013;218:61–9, http://dx.doi.org/10.1016/j.toxlet.2013.01.012.
[44] Zhang A, Sun H, Wu G, Sun W, Yuan Y, Wang X. Proteomics analysis of hepatoprotective effects for scoparone using MALDI-TOF/TOF mass spectrometry with bioinformatics. OMICS 2013;17:224–9, http://dx.doi.org/10.1089/omi.2012.0064.
[45] Sharanova NE, Kulakova SN, Baturina VA, Toropygin IY, Khriapova EA, Vasilyev AV, et al. Effect of coenzyme Q10 on the proteomic profile of the cytosolic and microsomal fractions from rat hepatocytes upon dietary consumption of various lipid components during ontogeny. Bull Exp Biol Med 2013;154:320–5.
[46] Bakala H, Ladouce R, Baraibar M.A., Friguet B. Differential expression and glycative damage affect specific mitochondrial proteins with aging in rat liver. Biochim Biophys Acta 2013;1832:2057–67, http://dx.doi.org/10.1016/j.bbadis.2013.07.015.
[47] Chapel A, Kieffer-Jaquinod S, Sagné C, Verdon Q, Ivaldi C, Mellal M, et al. An extended proteome map of the lysosomal membrane reveals novel potential transporters. Mol Cell Proteomics 2013;12:1572–88, http://dx.doi.org/10.1074/mcp.M112.021980.
[48] Gronemeyer T, Wiese S, Grinhagens S, Schollenberger L, Satyagraha A, Huber LA, et al. Localization of Rab proteins to peroxisomes: a proteomics and immunofluorescence study. FEBS Lett 2013;587:328–38, http://dx.doi.org/10.1016/j.febslet.2012.12.025.
[49] Benson WH, Di Giulio RT. Genomic approaches for cross-species extrapolation in toxicology. CRC Press; 2006.
[50] Wright JC, Beynon RJ, Hubbard SJ. Cross species proteomics. Methods Mol Biol 2010;604:123–35, http://dx.doi.org/10.1007/978-1-60761-444-9_9.
[51] Golizeh M, Schneider C, Ohlund L, Sleno L. Dataset from proteomic analysis of rat, mouse, and human liver microsomes and S9 fractions. Data Brief 2015, http://dx.doi.org/10.1016/j.dib.2015.02.007.
[52] Farrah T, Deutsch EW, Hoopmann MR, Hallows JL, Sun Z, Huang C-Y, et al. The state of the human proteome in 2012 as viewed through PeptideAtlas. J Proteome Res 2013;12:162–71, http://dx.doi.org/10.1021/pr301012j.
[53] Yang Y, Xiao Q, Humphreys WG, Dongre A, Shu Y. Identification of human liver microsomal proteins adducted by a reactive metabolite using shotgun proteomics. Chem Res Toxicol 2014;27:1537–46, http://dx.doi.org/10.1021/tx500181p.
[54] Tzouros M, Pähler A. A targeted proteomics approach to the identification of peptides modified by reactive metabolites. Chem Res Toxicol 2009;22:853–62, http://dx.doi.org/10.1021/tx800426x.
[55] Rombach EM, Hanzlik RP. Detection of adducts of bromobenzene 3,4-oxide with rat liver microsomal protein sulfhydryl groups using specific antibodies. Chem Res Toxicol 1999;12:159–63, http://dx.doi.org/10.1021/tx980177v.
[56] Shin N, Liu Q, Stamer SL, Liebler DC. Protein targets of reactive electrophiles in human liver microsomes. Chem Res Toxicol 2007;20:859–67, http://dx.doi.org/10.1021/tx700031r.